Pergamon

Solar Energy, Vol. 52, No. 4, pp. 337–346, 1994

0038-092X/94 $6.00 + .00

0038-092X(94)E0001-F

# SKY LUMINANCE DATA VALIDATION: COMPARISON OF SEVEN MODELS WITH FOUR DATA BANKS

PIERRE INEICHEN,*† BENOÎT MOLINEAUX,* and RICHARD PEREZ**†
*University of Geneva, GAP, 1231 Conches, Switzerland
**ASRC, State University of New York, Albany, NY, U.S.A.

**Abstract**—In order to insure the comparability of the data acquired within the International Daylight Measurement Program, we made a preliminary investigation on the behavior of four daylight data banks when compared with the predictions of seven sky luminance distribution models. We present, in this study, the results of these comparisons, focusing on the performance of the models depending on the site of measurements, the position of the point source of light within the sky, and the weather conditions. We obtain on the whole very similar results, independently of the instrument and the site of measurement, even with limited data banks that cannot be taken as representative of the various climates.

## 1. INTRODUCTION

In the field of interior design, a good knowledge of the energy and daylight availability is essential for an efficient use of these renewable resources. Solar radiation is measured in many stations throughout the world; this is not the case for daylight. In order to provide for this lack of data, the "Commission Internationale de l'Eclairage" (CIE) has organized an International Daylight Measurement Program (IDMP) with the objective of collecting worldwide data on daylight availability. In January 1993, IDMP regrouped 15 "research class stations" [21] around the world: 5 in Europe, 5 in Japan, 2 in the U.S., 2 in Asia, and 1 in Australia. We operate one such a station in Geneva, Switzerland, where we measure irradiance (global, diffuse, and beam), illuminance (global, diffuse, beam, and vertical) and luminance (zenith, sky).

The development and evaluation of luminous efficacy and sky luminance distribution models require measured values that are severely tested and validated. To achieve this goal, Molineaux and Ineichen [14] developed an effective automatic quality control procedure.

In this article, we are concerned with the performance of sky luminance models and with the quality of the data used for their evaluation. We present a preliminary investigation on the behavior of daylight data banks from four different countries when compared to the predictions of seven models. The results give a good idea of the quality and comparability of the daylight measurements being collected within IDMP, in view of a large-scale exchange of data.

## 2. DESCRIPTION OF THE SITES

We obtained a limited set of data from three other laboratories in Japan, the U.S., and Great Britain. For each data bank, we give, in Table 1, the location of the station, the number of days involved in this study, the time step of the acquisition, the measured parameters, and the type and manufacturer of the sensors. The measurements are independent (different manufacturers, different calibration of sensors, different methods of measurement, etc.) and cover a period of approximately 10 days with clear, intermediate, and overcast conditions. For Geneva, we chose a 9-day period in August 1992.

*Data from Japan*

The station is located in Koto-Ku, at Takenaka Corporation, Technical Research Laboratories. All the Japanese instruments are manufactured by EKO in Japan. The data bank includes 8 days of data, from May 12 to May 21, 1992. The measurements are taken every 30 min and are instantaneous values. The scan duration is 2 min 35 s; irradiances and illuminances are measured at the beginning of the scan [5].

*Data from the U.S.*

The data set was taken at Battelle Institute, Berkeley in 1985 and 1986 by J. Michalsky *et al.* [13] and reactualized by R. Perez *et al.* [16] at ASRC (Albany). The sky scanner is a homemade instrument by Kleckner *et al.* [8]; one scan consists of 186 points of measurement. Only the beam illuminance was simultaneously recorded during the data acquisition. The other illuminance and irradiance components are integrals or modeled values. We used 11 days of data from September 16 to September 31, 1985.

*Data from Great Britain*

The city of Garston is located 30 km northwest of London; the station is at the BRE (Building Research Establishment) and under the responsibility of P. Littlefair. As in Geneva, their sky scanner is manufactured by PRC Krochmann (During the analysis of BRE's

† ISES members.

Table 1. Data banks; location of the station, number of days involved in this study, time step of the acquisition, measured parameters, and type and manufacturer of the sensors

| Country | Japan | U.S.A. | Great Britain | Switzerland |
|---|---|---|---|---|
| City | Koto-Ku | Berkeley | Garston | Geneva |
| Institute | Takenaka Corp. | LBL | BRE | University |
| Latitude | 35.7°N | 37.9°N | 51.7°N | 46.2°N |
| Longitude | 139.8°E | 122.2°W | 0.4°W | 6.1°E |
| Altitude | 22 m | 396 m | 80 m | 400 m |
| Sky scanner | EKO | MASP (Battelle) | PRC Krochmann | PRC Krochmann |
| No. pts. per scan | 145 | 186 | 145 | 145 |
| No. days/no. scans | 8/203 | 11/423 | 9/257 | 9/376 |
| Time step | 30′ | 15′ | 15′ | 15′ |
| *Dvh* | EKO ML-010S | Scan integral | LMT | LiCor |
| *Bvn* | EKO ML-010SD | Sun luminance | LiCor + NIP tube | LiCor + NIP tube |
| *Gvh* | EKO ML-010S | *Dvh* + *Bvn* sin(hs) | LMT | PRC 910GV |
| *Bn* | EKO MS-52 | Luminous efficacy | NIP | NIP |
| *Gh, Dh* | EKO MS-801 | Luminous efficacy | CM11 | CM11 |
| Diffuse | Shadow band 5/50 | Scan integral | Shadow band 5/50 | Rotating disk |
| Vertical irradiances | NESW | — | NESW | — |
| Vertical illuminances | NESW | — | NESW | NESW |

data, Littlefair [11] noted the same problems as we had with our scanner described by Ineichen and Molineaux [14]). The diffuse components are measured with a 50 mm × 508 mm shadow band and are corrected using skies with nonuniform luminance distribution, including the CIE overcast and clear skies [11]. We have 9 days of data from August 20, 1991 to January 15, 1992.

*Data from Geneva*

To use a comparable set of data, we extracted from our data bank a 9-day data set from August 22, 1992 to September 1, 1992. Our instrument is a PRC sky scanner and we are recording instantaneous values every 15 min. The duration of the scan is 30 s and we are measuring the illuminance and irradiance components during the first 15 s of the scan. Our sensors are calibrated outdoors side by side against a LiCor and a CM10 substandard, which are calibrated, respectively, at the Institut de Métrologie (Berne, Switzerland) and at the World Radiation Centre (WRC, Davos, Switzerland).

## 3. INTERCOMPARISON OF THE DATA

The first step of our analysis was to test the coherence of the data. We compared the horizontal diffuse illuminance, *Dvh,* with the integral of the luminances over the hemisphere. For the integral, we took into account all luminance measurements for which the distance to the sun was greater than 6° (respectively, 144 and 185 measurements/scan). Considering that illuminances are easier to measure, and illuminance sensors easier to calibrate, we made the hypothesis that the value of *Dvh* was correct if the three basic illuminances (direct, global, and diffuse) were coherent with each other. As we noted some disparity between *Dvh* and the scan integral, we normalized the integral of the scan to the corresponding diffuse horizontal illuminance.

## 4. DESCRIPTION OF THE SKY LUMINANCE DISTRIBUTION MODELS

All the models used in this study (except the Perez model) are summarized in a publication from Perez *et al.* [17], Table 2 gives the input data, the governing parameters, etc., for each model.

*Brunger model*

The model is a three-component continuous model and was originally developed for modeling the sky radiance; it is a superposition of three distinct terms, isotropic, circumsolar, and horizontal brightening factor. The weighting parameters are *Dh/Gh* and the clearness index *Kt* [2].

*Matsuzawa model*

This model is a combination of the three CIE standard skies: clear, intermediate, and overcast. The governing parameter is an illuminance "cloud ratio" defined as *Dvh/Gvh* [12].

*ASRC–CIE model*

Perez *et al.* [17] modified Matsuzawa's model to take into account the high turbid intermediate skies. The interpolating parameters are Perez' epsilon and delta (clearness and brightness) coefficients. We reference here two versions of the model [15,17]; the best results are obtained with the most recent version, which was used in this study.

*Perez model*

Five coefficients describe the quality and the quantity of the luminance of the sky dome. Each of the coefficients has a specific physical effect and depends on epsilon and delta: (a) darkening or brightening of the horizon region; (b) luminance gradient near the horizon; (c) relative intensity of the circumsolar region; (d) width of the circumsolar region; and (e) the relative backscattered light [18].

Table 2. Sky luminance distribution models: Summary of the input data, governing parameters, and number of coefficients

| Model | Input | Geometry | Weighting parameter | Coefficients matrix |
|---|---|---|---|---|
| Brunger | *Gh, Dh, Dvh* | *Z, Io* | *K, Kt* | $4 \times (9 \times 9) = 324$ |
| Matsuzawa | *Gvh, Dvh* | *Z* | *Kv* | — |
| | | | CIE skies | |
| ASRC-CIE | *Gh, Bn* | *Z, Io* | Epsilon, delta | — |
| | | | CIE skies | |
| Perez | *Gh, Bn* | *Z, Io* | Epsilon, delta | $5 \times (8 \times 4) = 160$ |
| Perraudeau | *Gh, Dh* | *Z* | Nebulosity index | $5 \times 8 = 40$ |
| Kittler | *Bvn*, albedo | *Z, Ivo, Ma* | Illum. turbidity | — |
| Harrison | Opaque cloud cover (*Gh, Dh*)* | *Z* | Op. cloud cover (normalized *K*)* | — |

* When op. cloud cover not available. *Kt* = clearness index; $K = Dh/Gh$; $Kv = Dvh/Gvh$.

*Perraudeau model*

The formulation of the model is a product of three functions, depending respectively on the angular distance to the sun (zeta), the height of the considered point, and the sun height. The five discrete sky conditions are parameterized with a nebulosity index, which is a normalized cloud ratio [20].

*Harrison model*

The Harrison model needs an opaque cloud cover [3] to combine two basic luminance distributions: clear and cloudy sky. We used a normalized $Dh/Gh$ coefficient as opaque cloud cover.

*Kittler model*

Based on the light diffusion theory, the Kittler [9] model is a complex formula that calculates the absolute or relative sky luminance pattern. The governing parameter is the atmospheric illuminance turbidity.

## 5. COMPARING THE MODELS

The performance of each model is evaluated with the mean bias difference:

$$\text{MBD} = \frac{1}{N} \cdot \sum_{i=1}^{N} (\text{computed value}_i - \text{measured value}_i)$$

and the root mean square difference:

$$\text{RMS} = \sqrt{\frac{1}{N} \cdot \sum_{i=1}^{N} (\text{computed value}_i - \text{measured value}_i)^2}$$

both expressed in relative values (%). We used two methods to compare the performances of the models described above:

- *Relative comparison*: in this case, the sum or the average of the evaluated sky luminance points is normalized by a corresponding measured value. The mean bias difference (MBD) will always be zero. Considering the points near the horizon are as important as the points near the zenith (if one considers a vertical surface, the luminance from the zenith region becomes negligible) we normalize the calculated values with an average luminance (and not an integrated illuminance).
- *Absolute comparison*: for these comparisons, we use luminance values expressed in $\text{cd} \cdot \text{m}^{-2}$ and normalized by *Dvh*. The result will be a nonzero MBD, depending on the ability of the model to describe the climate.

In Table 3 we give the number of occurrences in the data banks involved in this study for each model parameter, for the sun height and Linke turbidity coefficient.

*All sky performance*

We first analyzed the behavior of the models with the available parameters. Fig. 1 represents the behavior of the models with 12 geometrical and meteorological parameters. Each figure represents the difference between computed and measured values ($C - M$) expressed in $\text{cd} \cdot \text{m}^{-2}$ versus the considered parameter. The abscissa is divided into bins; for each of them we represent the MBD (point) surrounded by $\pm 1$ standard deviation (SD) (line):

$$\text{SD} = \sqrt{\frac{1}{N-1} \cdot \sum_{i=1}^{N} [(C-M)_i - \overline{(C-M)}]}$$

All the calculated values are normalized by the mean luminance (relative comparison); we did not take into account the points near the horizon (6° of elevation for Koto-Ku, Garston, and Geneva; 10° for Berkeley) because of the nonuniformity of the horizon.

One can point out that, although the different models do not have the same overall performance, the dependence patterns are very similar and show that the bias becomes greater near the sun (cf. pt. azimuth, zeta, *Lvm* dependence graphs). All of these models were developed for values of zeta (angular distance between the considered point and the sun) greater than about 12° to 15°. It should also be noted that some of the error may be attributed to the instruments' nonzero field of view; because of the steep luminance gradient near the sun, and because of the possible stray light, the instrument will have a tendency to overestimate for points close to the sun's position.

Table 3. Number of occurrences of different sky conditions for the model parameters, sun height, and Linke turbidity coefficient

| | Bin 1 | Bin 2 | Bin 3 | Bin 4 | Bin 5 | Bin 6 | Bin 7 | Bin 8 | Bin 9 |
|---|---|---|---|---|---|---|---|---|---|
| Perez | | | | | | | | | |
| Epsilon | 1 → 1.065 | 1.065 → 1.23 | 1.23 → 1.5 | 1.5 → 1.95 | 1.95 → 2.8 | 2.8 → 4.5 | 4.5 → 6.2 | 6.2 → | |
| No. of occurrences | 645 | 39 | 55 | 81 | 107 | 168 | 117 | 47 | |
| Brunger | | | | | | | | | |
| *Kt* | 0 → 0.1 | 0.1 → 0.2 | 0.2 → 0.3 | 0.3 → 0.4 | 0.4 → 0.5 | 0.5 → 0.6 | 0.6 → 0.7 | 0.7 → 0.8 | 0.8 → 0.9 |
| No. of occurrences | 133 | 216 | 172 | 142 | 95 | 115 | 152 | 193 | 41 |
| *K* | 0.9 → 1 | 0.8 → 0.9 | 0.7 → 0.8 | 0.6 → 0.7 | 0.5 → 0.6 | 0.4 → 0.5 | 0.3 → 0.4 | 0.2 → 0.3 | 0.1 → 0.2 |
| No. of occurrences | 610 | 53 | 37 | 44 | 46 | 75 | 102 | 133 | 159 |
| ASRC-CIE | | | | | | | | | |
| Epsilon | 1 → 1.4 | 1.4 → 3 | 3 → 6 | 6 → | | | | | |
| No. of occurrences | 717 | 237 | 250 | 55 | | | | | |
| Matsuzawa | | | | | | | | | |
| *Kv* | 0 → 0.3 | 0.3 → 0.65 | 0.65 → | | | | | | |
| No. of occurrences | 214 | 281 | 764 | | | | | | |
| Perraudeau | | | | | | | | | |
| In | 0 → 0.05 | 0.05 → 0.2 | 0.2 → 0.7 | 0.7 → 0.9 | 0.9 → | | | | |
| No. of occurrences | 357 | 268 | 155 | 151 | 328 | | | | |
| Sun geometry | | | | | | | | | |
| Sun height | 6° → 15° | 15° → 25° | 25° → 35° | 35° → 45° | 45° → 55° | 55° → 65° | 65° → 75° | | |
| No. of occurrences | 296 | 218 | 181 | 202 | 287 | 33 | 42 | | |
| Sky conditions | | | | | | | | | |
| Linke turbidity | 1.75 → 2.25 | 2.25 → 2.75 | 2.75 → 3.25 | 3.25 → 3.75 | 3.75 → 4.25 | 4.25 → 4.75 | 4.75 → 5.25 | For epsilon > 6 | |
| No. of occurrences | 2 | 4 | 26 | 13 | 7 | 3 | 0 | | |

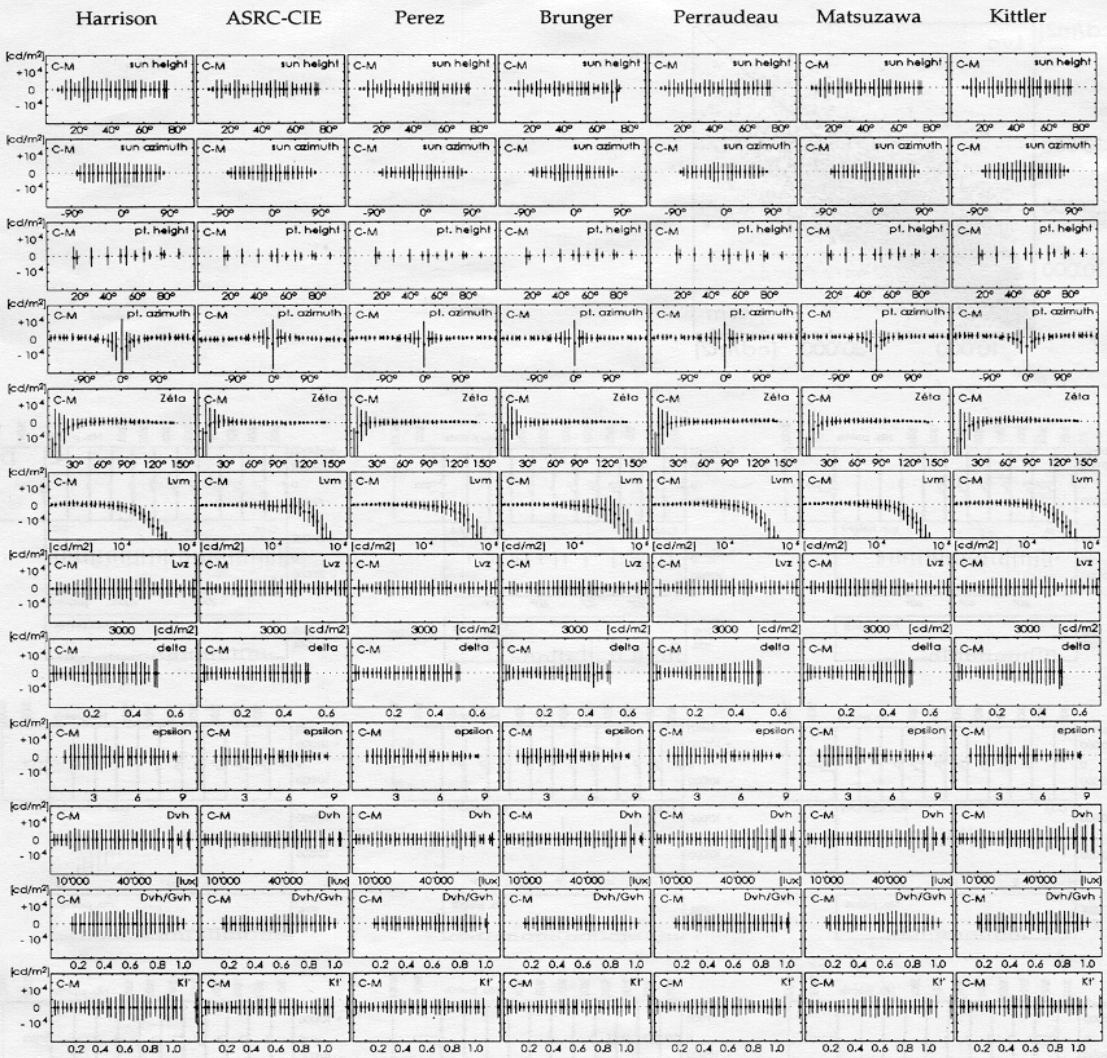


Fig. 1. Performance of seven models versus different parameters for all the stations. The luminance values are normalized by the mean luminance. The pt. azimuth is the angular distance between the azimuth of the point and the azimuth of the sun.

Considering the overall performances, two models give slightly better results: the Perez and Brunger models. We chose these two models for further analysis.

The detailed results obtained with the Perez model and data from all four sites are represented in Fig. 2. On the scatter-plot, one has the calculated values ($Lvc$) versus the corresponding measured values ($Lvm$). The diagonal line is representative of an ideal model. In order to underline the importance of the region near the sun, where the MBD and RMS become significant, we added histograms representing the number of considered points.

*Performance in four regions of the sky*

Using the MBD and SD indicators, we analyzed the behavior of the models for four different regions in the sky vault:

- the zenith region—all the points higher than 60° above the horizon (pt. height > 60°, ≈20% of the points);
- the "south" region—the region in the direction of the sun (pt. azimuth < 45° and pt. height < 60°, ≈20% of the points);
- the "north" region—the region opposite to the sun region (pt. azimuth > 135° and pt. height < 60°, ≈20% of the points); and
- the "east–west" region—the region on the left-hand side and the right-hand side of the sun (45° < pt. azimuth < 135° and pt. height < 60°, ≈40% of the points).

For all these cases, we normalize the integrated value of the scan to the diffuse illuminance ($Dvh$); we neither consider points within 15° of the sun, nor the points near the horizon.

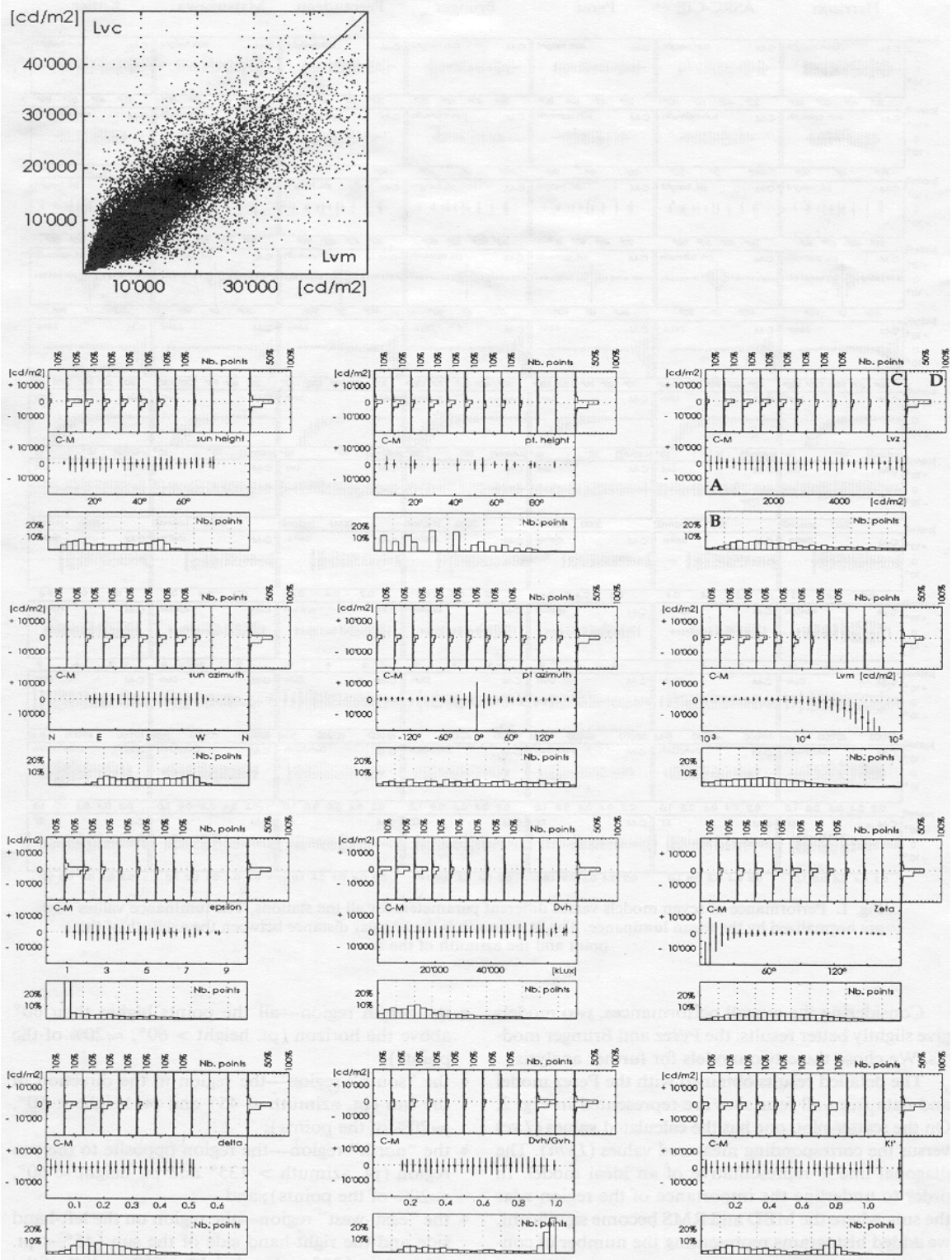


Fig. 2. Performance of the Perez model versus different parameters, for all the hemisphere and the four stations; the calculated luminance values are normalized by *Dvh*: (A) as in Fig. 1; (B) relative number of points for each of the 33 bins; (C) distribution of the MBD around the ideal model (MBD = 0), and each histogram is a compilation of three of the above bins; and (D) overall histogram of the distribution of the MBD.

Table 4. Mean bias difference (MBD) and root mean square difference (RMS) between model and measurements for the four stations and the seven models, for different normalizations, and cutting value for zeta with and without the horizon points

| Station | *Lvm* | Perez | | Brunger | | ASRC-CIE | | Matsuzawa | | Harrison | | Perraudeau | | Kittler | | Norm. | Horizon | Zeta |
|---|---|---|---|---|---|---|---|---|---|---|---|---|---|---|---|---|---|---|
| | | MBD | RMS | MBD | RMS | MBD | RMS | MBD | RMS | MBD | RMS | MBD | RMS | MBD | RMS | | | |
| Koto-Ku (203 scans) | 6991 | 5% | 48% | 2% | 45% | 3% | 53% | 3% | 57% | 5% | 48% | 14% | 65% | 2% | 58% | *Dvh* | With | >6° |
| | 7820 | −2% | 44% | −4% | 41% | −3% | 49% | −3% | 53% | −3% | 44% | 0% | 51% | −2% | 56% | *Dvh* | Without | >6° |
| | 7820 | — | 40% | — | 37% | — | 45% | — | 49% | — | 40% | — | 46% | — | 53% | *Lvm* | Without | >6° |
| | 7189 | — | 27% | — | 27% | — | 29% | — | 31% | — | 33% | — | 38% | — | 37% | *Lvm* | Without | >15° |
| Berkeley (423 scans) | 5493 | 0% | 42% | −3% | 48% | 0% | 45% | −3% | 51% | 0% | 59% | 4% | 52% | −3% | 53% | *Dvh* | With | >6° |
| | 5448 | 0% | 42% | 0% | 46% | 0% | 45% | −1% | 52% | 1% | 59% | 2% | 48% | −1% | 55% | *Dvh* | Without | >6° |
| | 5448 | — | 41% | — | 45% | — | 44% | — | 51% | — | 60% | — | 48% | — | 54% | *Lvm* | Without | >6° |
| | 5088 | — | 36% | — | 39% | — | 38% | — | 43% | — | 42% | — | 43% | — | 46% | *Lvm* | Without | >15° |
| Garston (257 scans) | 3184 | 3% | 46% | 1% | 54% | 1% | 54% | −1% | 67% | 5% | 79% | 11% | 53% | 5% | 51% | *Dvh* | With | >6° |
| | 2957 | 4% | 45% | 4% | 48% | 2% | 54% | 2% | 62% | 4% | 74% | 7% | 47% | 4% | 51% | *Dvh* | Without | >6° |
| | 2957 | — | 43% | — | 46% | — | 52% | — | 60% | — | 74% | — | 42% | — | 48% | *Lvm* | Without | >6° |
| | 2704 | — | 42% | — | 43% | — | 47% | — | 52% | — | 58% | — | 41% | — | 45% | *Lvm* | Without | >15° |
| Geneva (376 scans) | 5848 | 2% | 46% | −3% | 48% | 1% | 52% | 1% | 56% | 1% | 52% | 8% | 63% | 1% | 58% | *Dvh* | With | >6° |
| | 5967 | −1% | 46% | −2% | 47% | −2% | 49% | −2% | 53% | −2% | 51% | 1% | 56% | −2% | 56% | *Dvh* | Without | >6° |
| | 5967 | — | 44% | — | 45% | — | 48% | — | 51% | — | 51% | — | 51% | — | 53% | *Lvm* | Without | >6° |
| | 5421 | — | 40% | — | 42% | — | 42% | — | 43% | — | 45% | — | 45% | — | 46% | *Lvm* | Without | >15° |
| All stations (1259 scans) | 5381 | 2% | 46% | −1% | 48% | 1% | 51% | 0% | 57% | 2% | 57% | 8% | 60% | 0% | 57% | *Dvh* | With | >6° |
| | 5475 | 0% | 46% | −1% | 46% | −1% | 49% | −1% | 55% | 0% | 55% | 2% | 53% | −1% | 57% | *Dvh* | Without | >6° |
| | 5475 | — | 43% | — | 44% | — | 47% | — | 53% | — | 55% | — | 50% | — | 55% | *Lvm* | Without | >6° |
| | 5039 | — | 37% | — | 39% | — | 39% | — | 42% | — | 43% | — | 46% | — | 45% | *Lvm* | Without | >15° |

The results are presented in Table 4. One can see, in this table, that even if some of the models have a bias of approximately zero for the complete sky, this is not the case if we test different regions of the sky separately. The two previously selected models give the best description of the sky vault for all the considered regions.

Note that, as we previously observed, the SD remains high for all models. This is understandable because of the effect of "one-of-a-kind" cloud patterns that cannot be deterministically modeled. However, techniques are being developed to incorporate this "cloud noise" into a realistic model [1, 19].

## 6. SITE DEPENDENCE OF THE MODELS

Table 4 shows the results obtained when applying the seven models to the four limited data sets, for four different conditions:

- The scans are normalized by *Dvh* and evaluated over the whole hemisphere. This represents the overall performance of the model.
- The scans are normalized by *Dvh*, but without taking into account the first series of points above the horizon, in order to eliminate the effect of a nonideal horizon (in Geneva, we have a 6° high mountain in the southeast direction).
- The scans are normalized by the mean value of *Lvm* (MBD is zero), without the horizon. This is the intrinsic performance of the model.
- The same as above, but with cutting the points that are within 15° from the sun. This shows the circumsolar region influence on the model.

Fig. 3 is a graphical representation of the site dependence of Brunger's model. The graphs representing the dependence with the relative azimuth of the considered point (pt. azimuth) show a significant degradation of the MBD and the SD for the station of Garston and Geneva near the sun position (0° on the graphs). Concerning the data from Geneva, we know that the in-

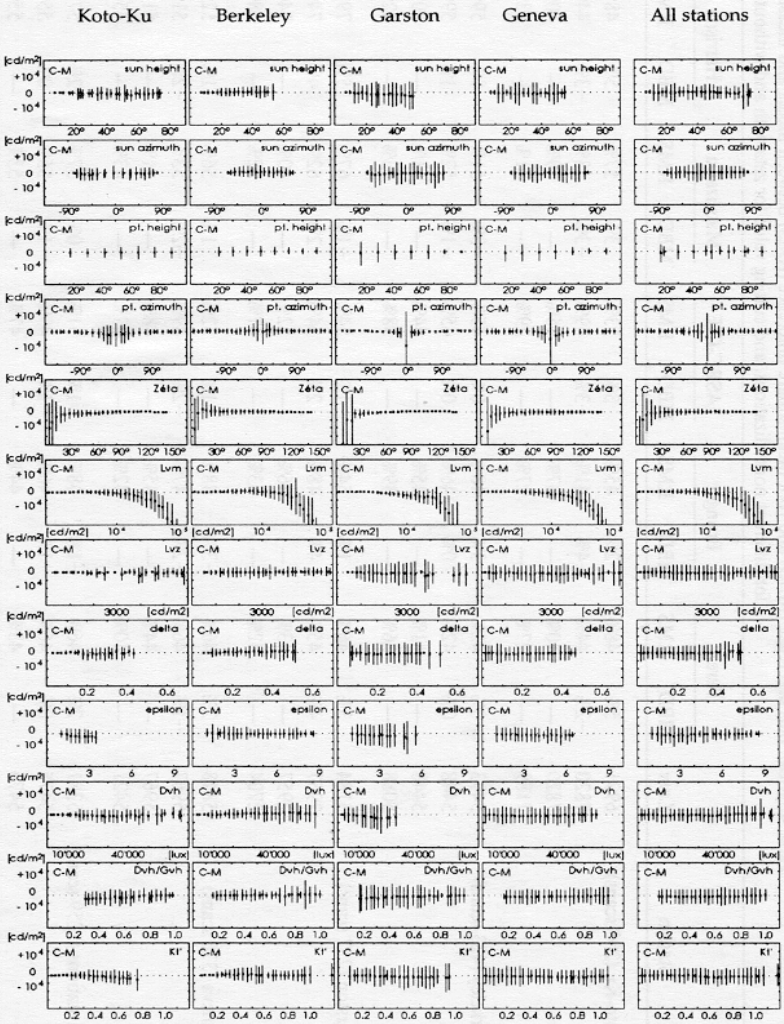


Fig. 3. Performance of the Brunger model versus different parameters, for the four stations; the luminance values are normalized by the mean luminance.

Table 5. Histograms of the models' performances for different sky regions. The first bar represents the overall performance, the other bars represent the four sky regions' performances (zenith, south, north, and east–west)

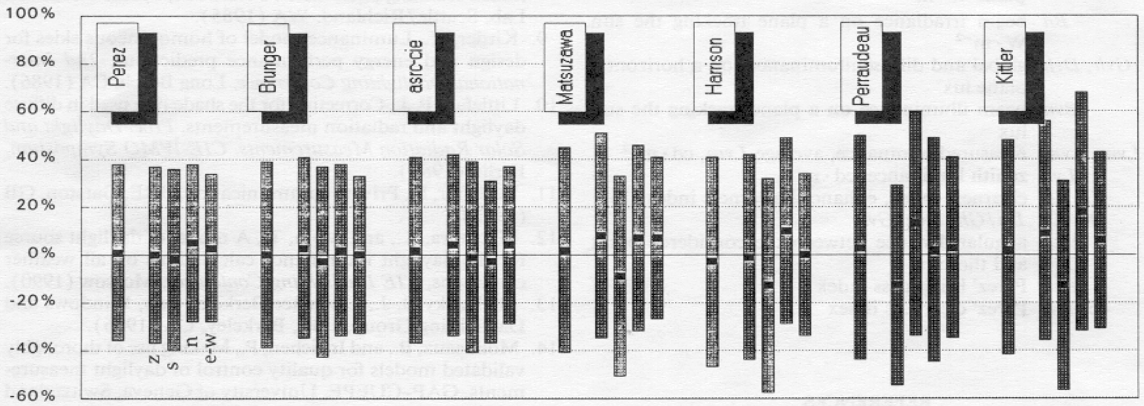


| Sky region | Nb Pt. | *Lvm* | Perez MBD | Perez SD | Brunger MBD | Brunger SD | ASRC-CIE MBD | ASRC-CIE SD | Matsuzawa MBD | Matsuzawa SD | Harrison MBD | Harrison SD | Perraudeau MBD | Perraudeau SD | Kittler MBD | Kittler SD |
|---|---|---|---|---|---|---|---|---|---|---|---|---|---|---|---|---|
| All sky | 153'655 | 5039 | 1% | 37% | 0% | 39% | 2% | 39% | 2% | 43% | −3% | 44% | 3% | 47% | 2% | 46% |
| Zenith | 30'966 | 5025 | 0% | 37% | 3% | 38% | 4% | 38% | 8% | 43% | −1% | 43% | −13% | 42% | 9% | 46% |
| South | 28'214 | 8302 | −2% | 38% | −3% | 40% | −1% | 40% | −9% | 42% | −13% | 45% | 13% | 47% | −13% | 43% |
| North | 30'659 | 3572 | 5% | 33% | 2% | 36% | −3% | 34% | 7% | 39% | 10% | 39% | 2% | 47% | 18% | 47% |
| East–west | 63'816 | 4309 | 3% | 31% | 0% | 33% | 4% | 33% | 7% | 34% | 0% | 34% | 3% | 38% | 6% | 37% |

All stations: zeta > 15° without horizon normalized by *Dvh*.

strument has errors in the positioning of the measurement head. The station of Garston is also equipped with a PRC Krochmann sky scanner.

The study of Table 4 and Fig. 3 shows that the seven models give better results with the Japanese data. The better performance obtained with the Perez model on Berkeley's data is due to the correlation between the data and the model development, and to the luminance integrated value of *Dvh*.

## 7. CONCLUSION

All the results presented are obtained with limited data banks, covering a small period of the year (no season, humidity, temperature, turbidity, etc., dependencies are considered here), and cannot be taken as representative of the various climates, but the aim of this study was to validate sky luminance distribution data banks. Nevertheless, from the figures and tables, one can see:

- For luminance values far from the sun direction, Koto-Ku's data gave the best results. This may be due to higher atmospheric turbidity (or lower epsilon values) in this data bank.
- As we did not find opaque cloud cover measurements for the tested data, we used a normalized $K$ index ($K = Dh/Gh$) to apply Harrison's model. The result is a great disparity of the results depending on the data bank.
- The smallest reductions in RMS when the circumsolar region was removed were obtained for the Garston and the Geneva data banks and may be due to the better optical system of the sky scanner: the PRC Krochmann scanner has a sensitivity equal to zero at ±5°, whereas the EKO Instruments scanner's sensitivity is 60% of the maximum at ±5°, going down to zero at ±9° [7]. Such a conclusion cannot be made from Berkeley's data, because all of the nonluminance data (except *Bvn*) are deduced from luminance measurements.
- According to the significant change in MBE and RMS, when eliminating the horizon band in the Japanese data, we conclude that the station was surrounded by obstructions with nonnegligible height.

On the whole, and without the climate's representative data, we obtained similar results, independently of the instrument and the site of measurement. We conclude that the different data banks are comparable.

*Acknowledgments*—This study was supported by the Swiss Federal Energy Office (OFEN). We thank P. Littlefair from the BRE and N. Igawa from Takenaka Corp. for providing the data. Collaboration with the State University of New York was possible thanks to support from the U.S. National Science Foundation (INT 9002363).

## NOMENCLATURE

*Io*, *Ivo* extraterrestrial irradiance and illuminance on a plane tracking the sun

| | |
|---|---|
| $Z$ | solar zenith angle |
| $Ma$ | optical air mass |
| $Gh$, $Dh$ | global and diffuse irradiances on a horizontal plane $W \cdot m^{-2}$ |
| $Bn$ | beam irradiance on a plane tracking the sun $W \cdot m^{-2}$ |
| $Gvh$, $Dvh$ | global and diffuse illuminances on a horizontal plane lux |
| $Bvn$ | beam illuminance on a plane tracking the sun lux |
| $Lvm$, $Lvm$ | measured luminance, average $Lvm$, $cd \cdot m^{-2}$ |
| $Lvz$ | zenith luminance, $cd \cdot m^{-2}$ |
| $Kt$, $Kt'$ | clearness index, enhanced clearness index [16] |
| $K$, $Kv$ | $Dh/Gh$, $Dvh/Gvh$ |
| zeta | angular distance between the considered point and the sun |
| delta | Perez' brightness index |
| epsilon | Perez' clearness index |

## REFERENCES


1. Beyer, H. G., Decker, B., Hammer, A., Luther, J., Poplawska, J., Steinberger-Willms, Stolzenburg, K., and Wieting, P., Analysis and synthesis of radiation data for the assessment of fluctuations in the power output of large PV-arrays, *Proceedings of the* 11*th E.C. Photovoltaic Solar Energy Conference,* Montreux, pp. 1652–1655 (1992).
2. Brunger, A. P., and Hooper, F. C., Anisotropic sky radiance model based on narrow field of view measurements of shortwave radiance, *Solar Energy* **51**(1), 53–64 (1993).
3. Combes, C. A., and Harrison, A. W., Radiometric estimation of cloud cover, *J. Atm. Oc. Technol.* **2**(4), 482–490 (1985).
4. Harrison, A. W., Directional sky luminance versus cloud cover and solar position, *Solar Energy* **46**(1), 13–19 (1991).
5. Igawa, N., Private communication, Takenaka Corp., Japan (1992).
6. Ineichen, P., and Molineaux, B., *PRC sky scanner characterisation, cosime dependence, aperture angle of NPB, honeycomb on PRC* 910*GV,* GAP–CUEPE, University of Geneva, 1231 Conches (1992).
7. Ineichen, P., and Molineaux, B., *Characterisation and comparison of two sky scanners: PRC Krochmann and EKO Instruments,* Internal report, Groupe of Applied Physics, University of Geneva, Switzerland (1993).
8. Kleckner, E. W., et al., *A multi-purpose computer-controlled scanning photometer,* PNL-4081, Pacific Northwest Lab, Seattle/Richland, WA (1985).
9. Kittler, R., Luminance model of homogeneous skies for design and energy performance predictions, 2*nd International Daylighting Conference,* Long Beach, CA (1986).
10. Littlefair, P. J., Correcting for the shade ring used in diffuse daylight and radiation measurements, *Proc. Daylight and Solar Radiation Measurements, CIE-WMO Symposium,* Berlin (1989).
11. Littlefair, P., Private communication, BRE, Garston, GB (1992).
12. Matsuura, K., and Iwata, T., A model of daylight source for the daylight illuminance calculations on all weather conditions, *CIE Daylighting Conference,* Moscow (1990).
13. Michalsky, J. J., Lawrence Berkeley Lab, Windows and Daylighting Group, LBL, Berkeley, CA (1986).
14. Molineaux, B., and Ineichen, P., Making use of thoroughly validated models for quality control of daylight measurements. GAP–CUEPE, University of Geneva, Switzerland (1993).
15. Perez, R., Ineichen, P., Seals, R., Michalsky, J., and Stewart, R., Modelling daylight availability and irradiance components from direct and global irradiance, *Solar Energy* **44**(5), 271–289 (1990).
16. Perez, R., Ineichen, P., Seals, R., and Zelenka, A., Making full use of the clearness index for parametrizing hourly insolation conditions, *Solar Energy* **45**(2), 111–114 (1990).
17. Perez, R., Michalsky, J., and Seals, R., Modelling sky luminance angular distribution for real sky conditions. Experimental evaluation of existing algorithms, *J. Illumin. Engg. Soc.* **21**(2), 84–92 (1992).
18. Perez, R., Seals, R., and Michalsky, J., An all-weather model for sky luminance distribution, *Solar Energy,* **50**(3), 235–245 (1993).
19. Perez, R., Seals, R., Michalsky, J., and Ineichen, P., Geostatistical properties and modeling of random clouds pattern for real skies, *Solar Energy* **51**(1), 7–18, 1993b.
20. Perraudeau, M., Daylight availability from energetic data, *CIE Daylighting Conference, Moscow,* Vol. I, pp. A17 (1990).
21. Tregenza, P. R., Perez, R., Michalsky, J., and Seals, R., Guide to recommended practice of daylight measurement, CIE TC-3.07, Final draft, August 1993.